Improved diagnostic accuracy of thallium-201 myocardial perfusion single-photon emission computed tomography with CT attenuation correction

Jei-Yie Huang, MD, MS,[a,b] Ruoh-Fang Yen, MD, PhD,[a] Wen-Chung Lee, PhD,[b] Chun-Kai Huang, MD,[b,c] Pei-Ying Hsu, MD,[d] Mei-Fang Cheng, MD,[a] Ching-Chu Lu, MD, MS,[a,b] Yen-Hung Lin, MD, PhD,[c] Kuo-Liong Chien, MD, PhD,[b,c] and Yen-Wen Wu, MD, PhD, F.E.S.C.[a,c,e,f,g]

[a] Department of Nuclear Medicine, National Taiwan University Hospital and National Taiwan University College of Medicine, Taipei City, Taiwan
[b] Institute of Epidemiology and Preventive Medicine, College of Public Health, National Taiwan University, Taipei City, Taiwan
[c] Department of Internal Medicine, National Taiwan University Hospital and National Taiwan University College of Medicine, Taipei City, Taiwan
[d] Department of Nuclear Medicine, National Taiwan University Hospital, Yun-Lin Branch, Douliu City, Yun-Lin County, Taiwan
[e] Department of Nuclear Medicine, Far Eastern Memorial Hospital, New Taipei City, Taiwan
[f] Cardiology Division of Cardiovascular Medical Center, Far Eastern Memorial Hospital, New Taipei City, Taiwan
[g] National Yang-Ming University School of Medicine, Taipei City, Taiwan

Received Oct 15, 2017; accepted Jan 18, 2018
doi:10.1007/s12350-018-1230-y

Background. **The benefits of attenuation correction (AC) in technetium-99m myocardial perfusion imaging (MPI) have been well established. However, the value of thallium (Tl-201) AC and routine computed tomography AC (CTAC) were less well established. The aims of this study were to evaluate the diagnostic performance of thallium (Tl-201) MPI with additional CTAC and to determine which participants would benefit most.**

Methods and Results. **A total of 108 consecutive patients who underwent Tl-201 MPI and received coronary angiography within 3 months were enrolled. Diagnostic performance was determined by sensitivity, specificity, and receiver operating characteristic curve analysis. Subgroup analyses were performed using gender and obesity. CTAC improved the area under the curve (0.84 vs. 0.77, $P = 0.037$ at patient level), primarily due to a significant improvement in specificity (0.78 vs. 0.57, $P = 0.013$) and no significant difference in sensitivity (0.79 vs. 0.82, $P = 0.75$). In subgroup analysis, CTAC was most helpful in obese subjects, men, and especially right coronary artery lesions.**

Conclusions. **CTAC significantly improved diagnostic performance primarily by increasing the specificity, and the improvements were significantly greater in obese patients and male patients. These findings suggest that CTAC should be applied to Tl-201 MPI as routine clinical practice. (J Nucl Cardiol 2019;26:1584–95.)**

Electronic supplementary material The online version of this article (https://doi.org/10.1007/s12350-018-1230-y) contains supplementary material, which is available to authorized users.

The authors of this article have provided a PowerPoint file, available for download at SpringerLink, which summarizes the contents of the paper and is free for re-use at meetings and presentations. Search for the article DOI on SpringerLink.com

Yen-Wen Wu and Kuo-Liong Chien contributed equally to this article.
Reprint requests: Yen-Wen Wu, MD, PhD, FESC, Cardiology Division of Cardiovascular Medical Center, Far-Eastern Memorial Hospital, No. 21, Sec. 2, Nanya S. Rd., Banciao Dist., New Taipei City 220, Taiwan; *wuyw0502@gmail.com*

1071-3581/$34.00

Key Words: Computed tomography attenuation correction • myocardial perfusion imaging • single-photon emission tomography • coronary artery disease

Abbreviations	
AC	Attenuation correction
CAD	Coronary artery disease
CTAC	Computed tomography attenuation correction
LAD	Left anterior descending coronary artery
LCx	Left circumflex coronary artery
MPI	Myocardial perfusion imaging
RCA	Right coronary artery
SPECT	Single-photon emission computed tomography
Tl-201	Thallium-201

See related editorial, pp. 1596–1598

INTRODUCTION

Myocardial perfusion imaging (MPI) is a well-established diagnostic tool to evaluate coronary artery disease (CAD), and is widely used to guide medical decisions such as when to use invasive coronary angiography (CAG).[1] However, attenuation artifacts are still an important issue, especially when using low-energy radiotracers.[2] Since the introduction of combined single-photon emission computed tomography/computed tomography (SPECT/CT) in 2005,[3] CT attenuation correction (CTAC) has been performed by converting Hounsfield units into attenuation coefficients, providing a high-resolution transmission map in a short time.[4] A lower radiation dose in SPECT/CT has also been achieved by reducing X-ray tube current and incorporating new reconstruction protocols.[5] In addition, CT can provide additional anatomic details such as coronary calcium and CT angiography.[6,7]

A recent meta-analysis summarized the evidence in favor of the use of attenuation correction (AC) MPI to detect CAD by demonstrating improved diagnostic accuracy after AC.[8] However, few studies have evaluated the effect of CTAC,[3,9-12] and only two have used thallium-201 (Tl-201).[3,13] In Taiwan, MPI is mainly performed using Tl-201 with dipyridamole stress because of the lower cost and single injection for stress-redistribution studies.[14] The multiple emission characteristics of Tl-201 increases the challenge of image acquisition,[15] and the majority of low-energy characteristic X-rays can cause additional problems in attenuation.[4] Moreover, scattered photons cannot be neglected as they account for 50% of all detected photons in typical Tl-201 MPI.[16,17]

Gender and body habitus may also cause significant attenuation. However, few studies have focused on this issue,[11,13,18-20] and only one study was performed with an Asian population.[11] Furthermore, over-correction has been reported, and small perfusion defects can be missed resulting in lower sensitivity.[3,9,11,20–22]

The aim of this study was to investigate whether additional CTAC could improve the diagnostic accuracy of Tl-201 MPI in conventional hybrid SPECT/CT by combining the interpretation of both CTAC and non-AC (NAC) images using CAG as the reference standard. In addition, the study aimed to determine which subjects may benefit most from CTAC.

METHODS

Study Design and Study Population

This study was approved by the Institutional Review Board and complied with the Declaration of Helsinki (Approval Number: 201106041RC). The need for written informed consent was waived due to the retrospective nature of the study. The diagnostic performance of Tl-201 MPI was retrospectively evaluated by comparing CTAC vs. NAC. A total of 2,603 consecutive patients (2,380 who underwent dipyridamole testing, 214 who underwent exercise stress testing, and nine who underwent dobutamine testing) were referred for MPI at the division of Nuclear Medicine, National Taiwan University Hospital Yun-Lin Branch from January 2008 to June 2009. The inclusion criteria were patients (1) with known or suspected CAD, (2) who underwent CTAC MPI, and (3) who received CAG within 3 months after MPI. The exclusion criteria were (1) missing CAG reports, (2) patients who did not undergo CTAC for technical reasons, and (3) duplicate patients. Finally, a total of 108 subjects were enrolled for further analysis (Figure 1).

MPI was performed on the Symbia T2 system (Siemens Medical Solutions Inc., Hoffman Estates, Illinois, USA), which utilized single dual-head SPECT/CT. Clinical data including age, gender, height, weight, subjective symptoms, medical history, risk factors for CAD, and treatment before MPI were surveyed and recorded at the time of the index MPI study. Medical records were reviewed for at least 2 years after MPI, and major adverse cardiac events (MACEs; cardiac death or nonfatal myocardial infarction) were also recorded.

Image Acquisition and Reconstruction

Standard dipyridamole, treadmill, and dobutamine stress Tl-201 MPI were performed based on the American Society of Nuclear Cardiology and the American Heart Association guidelines.[23] MPI was acquired at 5 minutes and again at 3 to 4 hours after an injection of 2.5-3 mCi Tl-201. Reinjections

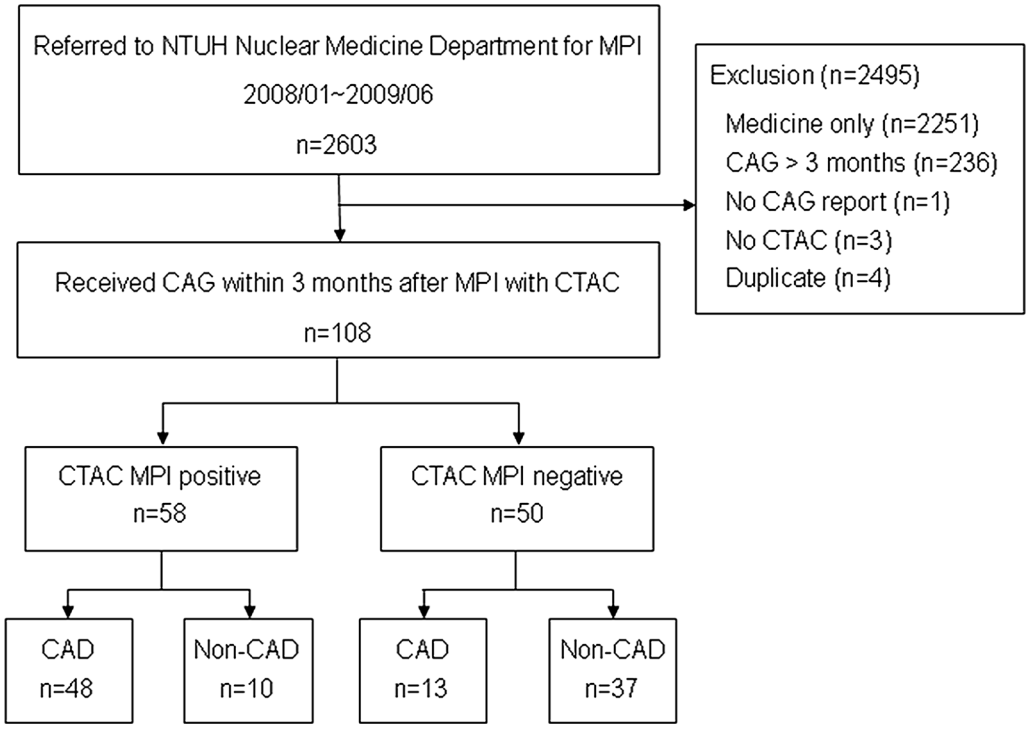

Figure 1. Study Flowchart. From January 2008 to June 2009, 2603 consecutive subjects were referred to our department for routine Tl-201 myocardial perfusion imaging. We excluded 2495 subjects according to exclusion criteria. A total of 108 subjects were enrolled in this study.

were performed if a severe perfusion defect was noted in the post-stress images. Electrocardiography (ECG)-gated SPECT (eight frames per cardiac cycle) was acquired on a dual-head SPECT/CT scanner equipped with low-energy general purpose collimators using a noncircular 180° acquisition for 64 projections at 22 (at stress) and 30 (at redistribution) seconds per projection. Two energy windows were set at 72 keV (± 15%) and 167 keV (± 10%) of Tl-201. Emission images were processed using Syngo imaging software (Siemens) and stored in a 128 × 128 matrix.[19,24]

A single low-dose breath-hold CT scan was performed after post-stress emission acquisition. In addition, a CT attenuation map was reconstructed by an average CT. Details of the acquisition protocols and parameters have been previously described.[19,24] CT images were reconstructed onto a 512 × 512 matrix. Attenuation maps were generated at both low and high energy spectrums, and attenuation coefficients were generated pixel by pixel. The emission and transmission images were manually matched to avoid misregistration artifacts.[11,25] Both NAC and CTAC emission images were processed using ordered-subset expectation maximization reconstruction software and displayed as previously described.[19,24]

Scatter correction was applied using a triple energy window method.[26] When using Tl-201, the correction was carried out using two sets of data: one set was acquired with a main window centered at photopeak energy (72 ± 15% and 167 ± 10% keV), and the other was acquired with two subwindows (20%) on both sides of the main window of 72 keV and one subwindow (15%) below the side of the main window of 167 keV. The number of scattered photons included in the main window was estimated from the counts acquired with the subwindows and then they are subtracted from the count acquired with the main windows.

Imaging Analysis

Two experienced nuclear medicine physicians (J-YH and Y-WW) interpreted the MPI images with consensus. The images were presented in a random sequence for interpretation by physicians who were blinded to the patient's history, CAG findings, and information from CT. The myocardium was divided into standardized AHA 17 segments, and each segment was scored in a semiquantitative manner using a standard 5-point scoring system.[27] The summed stress score (SSS), summed rest score, and summed difference score (SDS) were obtained. Left ventricle ejection fraction (LVEF) was calculated by quantitative-gated SPECT (version 7.0.7.3, Cedars Sinai Medical Center, Los Angeles, California, USA).[19] Non-perfusion abnormalities (transient left ventricle (LV) dilation, lung/heart ratio) and gated information (volume, ejection fraction, and wall motion) were not taken into account during perfusion scoring due to the assumption that these data would not be affected by AC.[28]

We calculated the Youden index for the optimal cutoff of SDS for further analyses.[29] An SDS of 5 was chosen as the

Table 1. Baseline characteristics of study population

	Total [mean (SD)]	CAD (+) $n = 61$	CAD (−) $n = 47$	*P* value
Age (years)	64.3 (10.5)	67.0 (9.9)	61.6 (10.7)	0.008
BMI	25.9 (4.18)	25.3 (4.4)	26.7 (3.8)	0.08
Post-stress LVEF (%)	52.8 (16.3)	49.8 (14.2)	56.6 (18.3)	0.039
Rest LVEF (%)	55.9 (16.2)	55.4 (14.6)	56.5 (18.4)	0.74
	n (%)			
Women	36 (33.3%)	27 (44.3%)	9 (19.1%)	0.008
Clinical history				
Hypertension	81 (75.0%)	52 (85.2%)	29 (61.7%)	0.007
DM	47 (43.5%)	31 (50.8%)	16 (34.0%)	0.12
Dyslipidemia	45 (41.7%)	30 (49.2%)	15 (31.9%)	0.08
Smoking	14 (13.0%)	6 (9.8%)	8 (17.0%)	0.24
History of CAD	49 (45.4%)	35 (57.4%)	14 (29.8%)	0.006
History of CABG	8 (7.4%)	7 (11.5%)	1 (2.1%)	0.13
History of HF	2 (1.9%)	0 (0%)	2 (4.3%)	0.19
History of VHD	1 (0.9%)	0 (0%)	1 (2.1%)	0.44
History of AAA/DAA	2 (1.9%)	1 (1.6%)	1 (2.1%)	1.00
Risk factors				
0 RF	0 (0.0%)	0 (0.0%)	0 (0.0%)	0.34
1RF	3 (2.8%)	2 (3.3%)	1 (2.1%)	
2RF	20 (18.5%)	7 (11.5%)	13 (27.7%)	
3RF	38 (35.2%)	22 (36.1%)	16 (34.0%)	
4RF	31 (28.7%)	20 (32.8%)	11 (23.4%)	
> 4RF	16 (14.8%)	10 (16.4%)	6 (12.8%)	

Data are represented as mean (SD) or number (percentages). Risk factors including hypertension, diabetes mellitus, dyslipidemia, current smoker, men ≥ 45 years old, or women ≥ 55 years old
AAA, Abdominal aortic aneurysm; *BMI*, body mass index; *CABG*, coronary artery bypass grafting; *CAD*, coronary artery disease; *DAA*, dissecting aortic aneurysm; *DM*, diabetes mellitus; *HF*, heart failure; *LVEF*, left ventricular ejection fraction; *RF*, risk factors; *VHD*, valvular heart disease

optimal cutoff for both CTAC and NAC images. Therefore, an SDS ≥ 5 was considered to be positive for CAD, and an SDS < 5 was considered to be negative for CAD. Assignment of vessel territory mainly followed the rule of standardized myocardial segmentation by the AHA Writing Group.[27] Because there was some overlap between coronary arteries, we allocated these perfusion abnormalities according to the CAG findings.[30,31] An abnormal MPI result in a certain coronary artery was defined when there was a difference in the summed segmental scores of a coronary artery territory between stress and resting images.

In addition, the diagnostic performances of CTAC non-ECG-gated and NAC with ECG-gated were compared in patients with good quality images of both CTAC and ECG-gated SPECT. LV functional parameters were used to differentiate scarred and attenuated myocardium.

Coronary Angiography

Invasive CAG was performed according to standard percutaneous techniques within 3 months after MPI. Clinical angiographic reports, based on visual interpretations by at least two experienced angiographers, were used as reference. Stenosis of 50% narrowing of the luminal diameter in the left main and stenosis of 70% narrowing in the left anterior descending coronary artery (LAD), left circumflex coronary artery (LCX), and right coronary artery (RCA) were considered to indicate significant stenoses.

Statistical Analysis

Descriptive analysis was performed according to CAD status. The Student's t-test and Fisher's exact test were used to compare differences between CAD-positive and CAD-negative groups, respectively. Semiquantitative data were expressed as mean ± SD. Comparisons between two groups (CTAC vs. NAC) were performed using the non-parametric paired samples *t*-test. The sensitivity, specificity, positive predictive value, negative predictive value, likelihood ratios, and their 95% confidence intervals for the diagnosis of CAD were calculated at patient level and by vascular territory. Differences in parameters between groups were compared using McNemar's test, weighted generalized score statistic, and Z test.[32] Receiver operating characteristic (ROC) curve analyses

Table 2. Diagnostic performance of stress myocardial perfusion imaging after CT-attenuated correction or not: by patient-based and vessel-based analyses

	CTAC (95% CI)	NAC (95% CI)	*P* value
Patient-based $n = 108$			
Sensitivity	0.79 (0.66, 0.88)	0.82 (0.70, 0.91)	0.75
Specificity	0.78 (0.64, 0.89)	0.57 (0.42, 0.72)	0.013
PPV	0.83 (0.71, 0.91)	0.71 (0.59, 0.82)	0.015
NPV	0.74 (0.60, 0.85)	0.71 (0.54, 0.85)	0.61
LR +	3.70 (1.48, 5.92)	1.93 (1.21, 2.65)	0.12
LR −	0.27 (0.13, 0.42)	0.31 (0.12, 0.51)	0.73
AUC	0.84 (0.76, 0.92)	0.77 (0.68, 0.86)	0.037
LAD $n = 108$			
Sensitivity	0.93 (0.82, 0.99)	0.93 (0.82, 0.99)	1.00
Specificity	0.56 (0.43, 0.69)	0.39 (0.23, 0.52)	0.001
PPV	0.61 (0.49, 0.73)	0.53 (0.42, 0.64)	<0.001
NPV	0.92 (0.79, 0.98)	0.89 (0.71, 0.98)	<0.001
LR +	2.15 (1.48, 2.82)	1.53 (1.18, 1.87)	0.09
LR −	0.12 (− 0.02, 0.25)	0.17 (− 0.03, 0.37)	0.68
AUC	0.75 (0.68, 0.82)	0.66 (0.59, 0.73)	<0.001
LCX $n = 108$			
Sensitivity	0.70 (0.51, 0.84)	0.73 (0.54, 0.87)	1.00
Specificity	0.76 (0.65, 0.85)	0.59 (0.47, 0.70)	<0.001
PPV	0.56 (0.40, 0.72)	0.43 (0.30, 0.58)	0.001
NPV	0.85 (0.74, 0.93)	0.83 (0.70, 0.92)	0.23
LR +	2.90 (1.48, 4.33)	1.76 (1.12, 2.40)	0.13
LR −	0.40 (0.17, 0.62)	0.46 (0.17, 0.76)	0.74
AUC	0.73 (0.64, 0.82)	0.66 (0.56, 0.75)	0.007
RCA $n = 106$			
Sensitivity	0.73 (0.56, 0.86)	0.84 (0.68, 0.94)	0.031
Specificity	0.70 (0.57, 0.80)	0.48 (0.36, 0.60)	0.001
PPV	0.56 (0.41, 0.71)	0.46 (0.34, 0.59)	0.012
NPV	0.83 (0.71, 0.91)	0.85 (0.69,0.94)	0.67
LR +	2.40 (1.36, 3.43)	1.61 (1.15, 2.06)	0.15
LR −	0.39 (0.16, 0.62)	0.34 (0.06, 0.62)	0.77
AUC	0.71 (0.62, 0.80)	0.66 (0.57, 0.74)	0.13

AUC, Area under receiver operating characteristic curve; *CTAC*, computed tomography attenuation correction; *LAD*, left anterior descending artery; *LCX*, left circumflex artery; *LR*, likelihood ratio; *LR +*, positive likelihood; *LR −*, negative likelihood; *NAC*, non-attenuation correction; *NPV*, negative predictive value; *PPV*, positive predictive value; *RCA*, right coronary artery

with areas under the curve (AUCs) were performed to evaluate the ability to predict significant coronary stenosis.

Additional subgroup analyses were performed, classified by gender and obesity. Obesity was defined as a body mass index (BMI) ≥ 27 kg/m^2 according to the criteria of the Ministry of Health and Welfare (MOHW) in Taiwan, and normal weight was defined as a BMI < 27 kg/m^2.[33] Interaction measurements and causal associations between gender and obesity and AC were calculated (Online Resource 1).

Sample size calculation was performed by comparing two ROC curves. The input data were the pooled estimates from four CTAC studies included in a previous meta-analysis,[8] and the sample size needed was 83. A two-sided P value < 0.05 was considered to be statistically significant. Statistical analysis was performed with commercial software (SAS version 9.4, SAS Institute Inc., North Carolina, USA and MedCalc for Windows, version 12.7, MedCalc Software, Ostend, Belgium).

RESULTS

Patients

A total of 108 patients [36 females (33.3%) and 72 males; mean age: 64.3 ± 10.5 years] were included in this study. No adverse events from MPI or CAG were

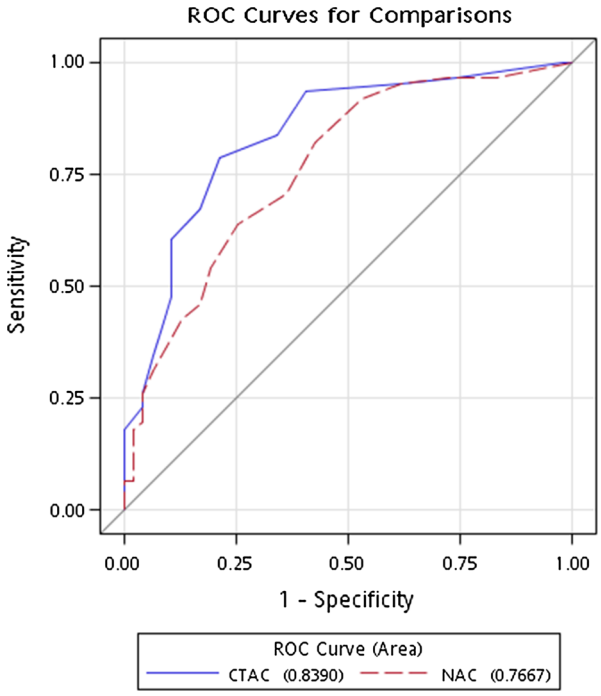

Figure 2. ROC curve plotting showed a significant improvement of AUCs after computed tomography attenuation correction ($P = 0.037$). (*AUC*, area under curve; *CTAC*, computed tomography attenuation correction, *NAC*, non-attenuation correction; *ROC*, receiver operating characteristic).

noted. The detailed clinical characteristics of the patients are summarized in Table 1, and MPI characteristics were are summarized in Online Resource 2. The average post-stress LVEF was 52.8%, and the rest LVEF was 55.9%.

Coronary Angiography Results

CAG showed significant coronary artery stenosis in 61 (56.5%) patients, with stenosis affecting LAD in 46 (42.6%), LCX in 33 (30.6%), and RCA in 37 (34.9%) patients. Of the patients with significant CAD, 23 (37.7%) had one-vessel disease, 21 (34.4%) had two-vessel disease, and 17 (27.9%) had three-vessel disease. CAG of the RCA was not performed in two patients due to technical failure; therefore, only 106 reference RCA angiographic results were analyzed.

Diagnostic Performance of MPI: CTAC vs. NAC

The mean SSS and SDS for CTAC were significantly lower than their respective values obtained with NAC (SSS: 13.58 ± 9.51 vs. 16.55 ± 9.58, $P < 0.0001$; SDS: 5.95 ± 5.06 vs. 7.12 ± 5.30, $P < 0.0001$,

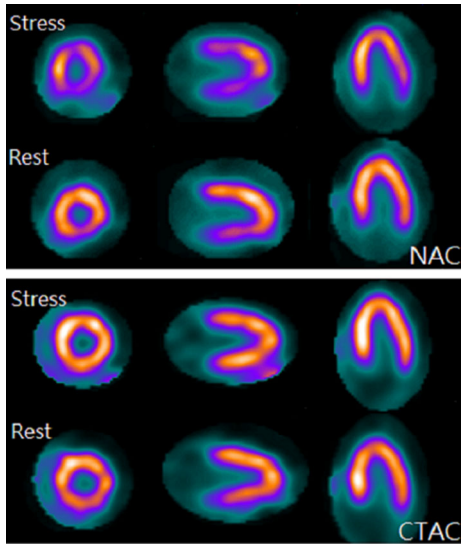

Figure 3. Representative myocardial perfusion imaging of a 57-year-old man with hypertension. Stress and rest images are shown for both non-attenuated corrected (NAC) vs. computed tomography attenuation correction (CTAC) images. The NAC image showed respiratory motion artifact. Mild reversible perfusion defects at the anterior, inferolateral, and inferior walls are noted on NAC image, which showed improvement in post-stress perfusion after CTAC. Coronary angiography 8 days later showed patent coronary arteries.

respectively). The three most attenuated segments were the basal inferior, basal inferolateral, and middle inferior segments.

The overall diagnostic performance of CTAC vs. NAC is shown in Table 2. There were no significant changes in sensitivity but significant improvements in specificity for detecting patient-level CAD, LAD, and LCX stenosis between CTAC vs. NAC, resulting in improvements in AUCs after CTAC. ROC curves for both CTAC and NAC (when used to diagnose CAD at the patient level) are shown in Figure 2. When using SDS ≥ 4 and SDS < 4 as cutoff values[34], the diagnostic performance between CTAC and NAC showed a similar trend, but the AUC failed to reach a significant difference ($P = 0.20$, Online Resource 3).

In the patients with RCA stenosis, CTAC significantly improved specificity ($P = 0.001$) but reduced sensitivity ($P = 0.031$), resulting in no change in AUC ($P = 0.13$). A demonstration of improved diagnosis after CTAC is shown in Figure 3 for patient #116.

Suboptimal gated SPECT imaging quality and inaccurate gated volumetric information were noted in 17 patients (15.7%), probably due to low Tl-201 count or gating errors. The diagnostic performance of CTAC non-ECG-gated was compared with NAC with ECG-gated in 91 patients with interpretable image quality of

Table 3. Diagnostic performance of stress myocardial perfusion imaging: CTAC non-ECG-gated vs. NAC with ECG-gated, by patient-based analyses

n = 91	CTAC non-ECG-gated (95%CI)	NAC with ECG-gated (95%CI)	*P* value
Sensitivity	0.80 (0.66, 0.89)	0.61 (0.47, 0.74)	0.0213
Specificity	0.82 (0.65, 0.92)	0.78 (0.62, 0.90)	1.00
AUC	0.80 (0.72, 0.89)	0.70 (0.60, 0.79)	0.0496

AUC, Area under receiver operating characteristic curve; *CTAC*, computed tomography attenuation correction; *ECG*, electrocardiography; *NAC*, non-attenuation correction

gated SPECT. The CTAC non-ECG-gated images showed better sensitivity (0.80 vs. 0.61, $P = 0.021$), similar specificity (0.82 vs. 0.78, $P = 1.00$), and borderline better AUC (0.80 vs. 0.70, $P = 0.0496$) compared with NAC with ECG-gated images (Table 3).

Subgroup Analysis

Subgroup analysis by gender showed similar results in males compared with the group as a whole (i.e., males plus females), as shown in Table 4A. CTAC showed a decrease in sensitivity only when diagnosing RCA stenosis, although this did not reach statistical significance (0.71 vs. 0.82, $P = 0.50$). However, in the female subgroup, although similar trends were noted (i.e., improvements in specificity and AUC at the patient level and for each vessel stenosis), the results failed to reach significance. Regarding the test of effect modification, no interaction between gender and AC was found at the patient level, LAD, LCX, or RCA ($P = 0.93$, 0.59, 0.41, 0.89, respectively).

In subgroup analysis by obesity versus normal weight, one patient did not have data on body height and body weight, and, therefore, BMI was not calculated. There were 38 patients in the obesity subgroup and 69 patients in the normal weight subgroup. Two patients did not have angiographic data of RCA (one in each subgroup).

Significant differences were noted in specificity and AUC between CTAC and NAC in both subgroups to diagnose patient-level CAD and LAD stenosis. However, when diagnosing LCX stenosis, the only result which reached significance was a change in specificity in the obesity subgroup. Moreover, when diagnosing RCA stenosis, significant differences were noted in specificity and AUC between CTAC and NAC only in the obesity subgroup. To test the effect modification, an interaction between BMI and AC was noted when diagnosing RCA stenosis ($P = 0.013$). Detailed information is shown in Table 4B.

DISCUSSION

AC vs. NAC

When diagnosing CAD at the patient level, the combination of CTAC images led to significant improvements in diagnostic performance by improving specificity without reducing sensitivity. When diagnosing single vessel stenosis, CTAC images significantly improved diagnostic performance when evaluating LAD and LCX, but only slightly improved diagnostic performance when evaluating RCA. The same results were noted in men at both patient and vascular levels. CTAC improved diagnostic performance in patient-level CAD and LAD stenosis regardless of weight. There was an interaction between BMI and RCA lesions and an improvement in the AUC of RCA stenosis only in the obesity subgroup.

Many reports in the literature have evaluated CTAC in MPI with diverse analytic methods. Our previous meta-analysis revealed that AC increased specificity without compromising sensitivity, resulting in an improvement in the diagnostic odds ratio.[8] In 2003, Utsunomiya et al. conducted the first CTAC study on Tl-201 MPI with a self-combined SPECT/CT system.[3] They found higher specificity and accuracy with CTAC images compared with NAC images at the patient level, and the difference in diagnostic accuracy was statistically significant ($P = 0.03$). The diagnostic accuracy was significantly higher with the CTAC images because of increased specificity when evaluating the RCA, whereas no significant differences were noted between CTAC and NAC images in the LAD and LCX territories. The clinical setting of the study by Utsunomiya et al. was very similar to our study, as we both used the same radiopharmaceutical and conducted our studies in an Asian population. However, their SPECT/CT was self-combined, whereas commercialized hybrid SPECT/CT is currently used in clinical practice.

Huang et al. evaluated the effect of CTAC on technetium-99m (Tc-99m) MPI in Chinese subjects,[11] and showed that CTAC increased specificity and

Table 4. Subgroup analyses of (A) gender and (B) body mass index

(A)	Men (n = 72)			Women (n=36)		
	CTAC	NAC	*P* value	CTAC	NAC	*P* value
Patient base						
Sensitivity (95% CIs)	1.00 (0.90, 1.00)	1.00 (0.90, 1.00)	1.00	0.93 (0.76, 0.99)	0.93 (0.76, 0.99)	1.00
Specificity	0.61 (0.43, 0.76)	0.37 (0.22, 0.54)	0.004	0.67 (0.30, 0.93)	0.44 (0.14, 0.79)	0.50
AUC	0.80 (0.72, 0.88)	0.68 (0.61, 0.76)	0.001	0.80 (0.63, 0.97)	0.69 (0.51, 0.86)	0.13
LAD						
Sensitivity	0.96 (0.80,1.00)	0.96 (0.80,1.00)	1.00	0.90 (0.70, 0.99)	0.90 (0.70, 0.99)	1.00
Specificity	0.60 (0.44,0.74)	0.40 (0.26, 0.56)	0.004	0.47 (0.21, 0.73)	0.33 (0.12, 0.62)	0.50
AUC	0.78 (0.70, 0.86)	0.68 (0.60, 0.76)	0.001	0.69 (0.54, 0.83)	0.62 (0.48, 0.76)	0.14
LCX						
Sensitivity	0.59 (0.33, 0.82)	0.59 (0.33, 0.82)	1.00	0.81 (0.54, 0.96)	0.88 (0.62, 0.98)	1.00
Specificity	0.78 (0.65, 0.88)	0.60 (0.46, 0.73)	0.002	0.70 (0.46, 0.88)	0.55 (0.32, 0.77)	0.25
AUC	0.69 (0.55, 0.82)	0.59 (0.46, 0.73)	<0.001	0.76 (0.61, 0.90)	0.71 (0.57, 0.85)	0.40
RCA	(n = 70)			(n = 36)		
Sensitivity	0.71 (0.44, 0.90)	0.82 (0.57, 0.95)	0.50	0.75 (0.51, 0.91)	0.85 (0.62, 0.97)	0.50
Specificity	0.68 (0.54, 0.80)	0.45 (0.32, 0.60)	<0.001	0.75 (0.48, 0.93)	0.56 (0.30, 0.80)	0.25
AUC	0.69 (0.56, 0.82)	0.64 (0.52, 0.75)	0.27	0.75 (0.60, 0.90)	0.71 (0.56, 0.86)	0.47
(B)	**BMI ≥ 27 (n = 38)**			**BMI < 27 (n = 69)**		
	CTAC	NAC	*P* value	CTAC	NAC	*P* value
Patient base						
Sensitivity (95% CIs)	0.95 (0.74, 1.00)	0.95 (0.74, 1.00)	1.00	0.98 (0.87, 1.00)	0.98 (0.87, 1.00)	1.00
Specificity	0.58 (0.34, 0.80)	0.26 (0.09, 0.51)	0.001	0.67 (0.46, 0.83)	0.48 (0.29, 0.68)	0.06
AUC	0.76 (0.64, 0.89)	0.61 (0.49, 0.72)	0.001	0.82 (0.73, 0.92)	0.73 (0.63, 0.83)	0.015
LAD						
Sensitivity	0.87 (0.60, 0.98)	0.87 (0.60, 0.98)	1.00	0.97 (0.83, 1.00)	0.97 (0.83, 1.00)	1.00
Specificity	0.48 (0.27, 0.69)	0.22 (0.07, 0.44)	0.031	0.63 (0.46, 0.78)	0.50 (0.33, 0.67)	0.06
AUC	0.67 (0.54, 0.81)	0.54 (0.42, 0.67)	0.005	0.80 (0.72, 0.88)	0.73 (0.65, 0.82)	0.018
LCX						
Sensitivity	0.38 (0.09, 0.76)	0.38 (0.09, 0.76)	1.00	0.80 (0.59, 0.93)	0.84 (0.64, 0.95)	1.00
Specificity	0.77 (0.58, 0.90)	0.50 (0.31, 0.69)	0.008	0.75 (0.60, 0.87)	0.64 (0.48, 0.78)	0.06
AUC	0.57 (0.38, 0.77)	0.56 (0.36, 0.76)	0.97	0.78 (0.67, 0.88)	0.74 (064, 0.84)	0.24
RCA	(n = 37)			(n = 68)		
Sensitivity	0.78 (0.40, 0.97)	0.78 (0.40, 0.97)	1.00	0.71 (0.51, 0.87)	0.86 (0.67, 0.96)	0.13
Specificity	0.71 (0.51, 0.87)	0.39 (0.21,0.59)	0.004	0.70 (0.53, 0.83)	0.55 (0.38, 0.71)	0.031
AUC	0.75 (0.58, 0.91)	0.59 (0.41, 0.76)	<0.001	0.71 (0.60, 0.82)	0.70 (0.60, 0.81)	0.94

AUC Area under receiver operating characteristic curve; *CTAC*, computed tomography attenuation correction; *LAD*, left anterior descending artery; *LCX*, left circumflex artery; *NAC*, non-attenuation correction; *RCA*, right coronary artery

accuracy at the patient level and increased specificity in the RCA territory, but decreased specificity in the LAD territory. In addition, Sharma et al. found that CTAC tended to increase the AUC of Tc-99m MPI, but without reaching statistical significance.[9] Masood et al. analyzed the effect of CTAC on Tc-99m MPI as interpreted by four readers,[12] and found that AC improved diagnostic performance. Interestingly, the readers who were prone to high sensitivity had the greatest gain in normalcy rate, whereas the reader prone to higher specificity had improvements in sensitivity and specificity. This suggests that improvement in one diagnostic variable was not inevitably associated with worsening of other variables.

Other studies comparing the diagnostic performance of AC vs. NAC have shown statistically significant differences between the two while others have not. However, they have all shown a similar trend of improved specificity and improved overall diagnostic performance at the patient level with AC.[3,8,9,11,12]

Gated vs. AC

In 2004, Johansen et al. reported that additional AC led to changes in the diagnosis on gated MPI.[35] Genovesi et al. compared AC with gated MPI and showed better diagnostic accuracy with gated MPI in the whole group, but that AC significantly improved specificity in identifying RCA stenosis in overweight men,[10] which is consistent with our study. On the other hand, Benkiran et al. reported that although both CTAC and gated MPI allowed for significant gains in specificity and diagnostic accuracy compared with NAC images in patients with a low prevalence of CAD, gated MPI provided more significant improvements compared with CTAC.[36] Consequently, Links et al. reported that the combination of gated MPI and AC was the best option for analysis.[37] However, these studies mainly used Tc-99m agents. Due to special characteristics of Tl-201, gated MPI in some patients may show poor image quality, less reliable quantitative assessments, and less reproducibility. In our study, 15.7% patients lacked gated information. For patients with both additional gated and CTAC information, CTAC and gated MPI showed similar diagnostic performances.

More recently, although cadmium-zinc-telluride (CZT)-based cameras had better physical performance and image quality with fewer artificial perfusion defects, ECG-gated SPECT can be used in routine clinical practice without increasing tracer dose or acquisition time.[38,39] However, conventional SPECT scanners are still widely used. To better predict CAD, the usefulness of CTAC on conventional SPECT, and especially with Tl-201 as the tracer, should be emphasized. In addition, conventional SPECT and CZT-based cameras have different attenuation artifact patterns,[40,41] so that interpretation should be made with caution and additional AC may be required.

Effect of CTAC

The current study showed a statistically significantly better diagnostic performance after CTAC in LAD and LCX territories. Although there was an improvement in the AUC after CTAC in the RCA territory, the difference was not statistically significant, which may be due to opposing changes in sensitivity and specificity. Previous studies have shown an improvement in diagnostic performance mostly when detecting RCA stenosis, and some have even shown a decline in detecting LAD stenosis.[3,11] The discordance between our study and previous studies with regard to the LAD and RCA territories could be due to lesser sub-diaphragmatic uptake in Tl-201 studies. In addition, normal physiological thinning of apical myocardium could contribute to this error. Apical thinning could be enhanced after AC, resulting in relatively less AC in the apical region compared with the rest of the left ventricular myocardium.[9,21] Most previous studies have only interpreted AC images, whereas we interpreted a combination of CTAC and NAC images together. Although scatter correction may cause deterioration of signal-to-noise ratio and reduce specificity, the simultaneous use of AC and scatter correction has been reported to improve the uniformity of myocardial perfusion uptake and reduce the drawback of over-correction of the inferior wall.[17] Therefore, we used scatter correction for image reconstruction of Tl-201 SPECT/CT in the current study.

Gender and Obesity

In the current study, the effect of CTAC was more significant in men compared with women, which is consistent with previous studies using CTAC or radionuclide AC.[11,13] A BMI of 27 was used as the cutoff value to define obesity as this value is used by the MOHW in Taiwan.[33] Although we used a different cutoff value, our results showed the same trend as in Western countries which use a BMI of 30 as the cutoff value.[20] Obesity significantly compromised the diagnostic accuracy of NAC images in patients with LAD or LCX stenosis in the current study, and AC was more useful in patients with a large body surface area or BMI in whom photonic attenuation was more significant. Gated acquisition with LV function assessment has been shown to provide additional functional information which can aid in differentiating soft tissue attenuation from true perfusion

defects.[10,42] Consequently, consistent with the study by Genovesi et al,[10] our study showed that CTAC is likely to be more useful in men and obese participants, especially in the RCA territory.

Strengths

This is the first study to evaluate the diagnostic performance of CTAC MPI with Tl-201 as perfusion radiopharmaceutical with a commercialized hybrid SPECT/CT scanner. Sample size estimation was done to ensure sufficient sample size. ROC curve analysis rather than simple sensitivity and specificity was used to determine the diagnostic performance.[43] Although Tl-201 is used less frequently in Europe and the US, it is still commonly used in most Asian countries, including Taiwan.[14] Attenuation artifacts may be more pronounced with this lower energy radiotracer. Scatter correction may also improve the diagnostic performance of MPI.[44,45] The SPECT/CT system used for MPI in our study performed spontaneous scatter correction. Our study also confirmed that single CT is clinically feasible for AC, with reasonable reductions in both radiation dose and scan time.

Limitations

This study was a community hospital-based study and only participants with suspected CAD were referred for MPI. Verification bias was a problem. Although patients with mild perfusion defects or equivocal findings may not have received CAG, all of the patients were clinically followed for at least 2 years. Our results suggest that CTAC is useful in making a differential diagnosis of scarred or attenuated myocardium in equivocal NAC results, and may decrease the usage of unnecessary CAG. Due to our study design, we were unable to perform head-to-head comparisons of sensitivity or specificity between NAC and CTAC. Multivessel disease was rather common in our patients, which may have led to an underestimation of the perfusion abnormality due to balanced ischemia. MPI can detect microvascular or diffuse diseases which may be underdiagnosed by CAG. Intravascular ultrasound or fractional flow reserve was not performed which may partly explain the discrepancy between MPI and CAG. Blinded interpretation may have led to an underestimation of the improvement in accuracy. The gated information was obtained from NAC data because of default setting. Patients with arrhythmia or severe motion artifacts may have compromised the diagnostic performance of Tl-201 ECG-gated MPI. However, this represents a real-world scenario.[46] We did not incorporate gated SPECT parameters with CTAC MPI results which may have provided incremental diagnostic value.[47] Few patients (18 patients) had a BMI above 30, and therefore the usefulness of CTAC in grade 2 and 3 obesity could not be established. Finally, this study only demonstrated the diagnostic performance of MPI; neither treatment response nor prognosis was evaluated.

CONCLUSION

CTAC MPI showed significant improvements in specificity and no significant changes in sensitivity for detecting CAD in patient level, and LAD, LCX stenosis in vessel level, compared with NAC images. CTAC non-ECG-gated images showed better sensitivity, similar specificity, and borderline better overall diagnostic accuracy comparing with NAC with ECG-gated images. This study further confirmed greater improvement after CTAC in obese patients and male patients, especially for RCA disease. These findings suggest that CTAC should be routinely applied to Tl-201 MPI when diagnosing CAD.

NEW KNOWLEDGE GAINED

Additional CTAC improved diagnostic certainty of Tl-201 MPI, especially with regard to specificity. Simultaneous CTAC and NAC image acquisition should be applied routinely if available, or at least in male and obese patients. Interpretation of CTAC and NAC images combined together can lead to more accurate results and appropriate treatment plans.

Acknowledgments

We gratefully acknowledge the assistance of Ms. Yu-Shuan Hung, Ms. Shu-Mei Lin, Ms. Hsiao-Fang Chou, and Ms. Wan-Li Wang for clinical data collection and imaging processing and analysis.

Disclosure

This study was supported in part by the Ministry of Science and Technology of Taiwan (100-2314-B-002-158, 101-2314-B-418-012-MY3, 106-2314-B-002-049-MY3). Jei-Yie Huang, Ruoh-Fang Yen, Wen-Chung Lee, Chun-Kai Huang, Pei-Ying Hsu, Mei-Fang Cheng, Ching-Chu Lu, Yen-Hung Lin, Kuo-Liong Chien, and Yen-Wen Wu declare that they have no conflict of interest.

References

1. Hendel RC, Berman DS, Di Carli MF, Heidenreich PA, Henkin RE, Pellikka PA, et al. ACCF/ASNC/ACR/AHA/ASE/SCCT/SCMR/SNM 2009 appropriate use criteria for cardiac radionuclide

imaging: a report of the American College of Cardiology Foundation Appropriate Use Criteria Task Force, the American Society of Nuclear Cardiology, the American College of Radiology, the American Heart Association, the American Society of Echocardiography, the Society of Cardiovascular Computed Tomography, the Society for Cardiovascular Magnetic Resonance, and the Society of Nuclear Medicine. J Am Coll Cardiol. 2009;53:2201–29.
2. Burrell S, MacDonald A. Artifacts and pitfalls in myocardial perfusion imaging. J Nucl Med Technol. 2006;34:193–211.
3. Utsunomiya D, Tomiguchi S, Shiraishi S, Yamada K, Honda T, Kawanaka K, et al. Initial experience with X-ray CT based attenuation correction in myocardial perfusion SPECT imaging using a combined SPECT/CT system. Ann Nucl Med. 2005;19:485–9.
4. Patton JA, Turkington TG. SPECT/CT physical principles and attenuation correction. J Nucl Med Technol. 2008;36:1–10.
5. Caobelli F, Kaiser SR, Thackeray JT, Bengel FM, Chieregato M, Soffientini A, et al. IQ SPECT allows a significant reduction in administered dose and acquisition time for myocardial perfusion imaging: evidence from a phantom study. J Nucl Med. 2014;55:2064–70.
6. Patchett ND, Pawar S, Miller EJ. Visual identification of coronary calcifications on attenuation correction CT improves diagnostic accuracy of SPECT/CT myocardial perfusion imaging. J Nucl Cardiol. 2017;24:711–20.
7. Schaap J, Kauling RM, Boekholdt SM, Nieman K, Meijboom WB, Post MC, et al. Incremental diagnostic accuracy of hybrid SPECT/CT coronary angiography in a population with an intermediate to high pre-test likelihood of coronary artery disease. Eur Heart J Cardiovasc Imaging. 2013;14:642–9.
8. Huang JY, Huang CK, Yen RF, Wu HY, Tu YK, Cheng MF, et al. Diagnostic performance of attenuation-corrected myocardial perfusion imaging for coronary artery disease: a systematic review and meta-analysis. J Nucl Med. 2016;57:1893–8.
9. Sharma P, Patel CD, Karunanithi S, Maharjan S, Malhotra A. Comparative accuracy of CT attenuation-corrected and non-attenuation-corrected SPECT myocardial perfusion imaging. Clin Nucl Med. 2012;37:332–8.
10. Genovesi D, Giorgetti A, Gimelli A, Kusch A, D'Aragona Tagliavia I, Casagranda M, et al. Impact of attenuation correction and gated acquisition in SPECT myocardial perfusion imaging: results of the multicentre SPAG (SPECT Attenuation Correction vs Gated) study. Eur J Nucl Med Mol Imaging. 2011;38:1890–8.
11. Huang R, Li F, Zhao Z, Liu B, Ou X, Tian R, et al. Hybrid SPECT/CT for attenuation correction of stress myocardial perfusion imaging. Clin Nucl Med. 2011;36:344–9.
12. Masood Y, Liu YH, Depuey G, Taillefer R, Araujo LI, Allen S, et al. Clinical validation of SPECT attenuation correction using x-ray computed tomography-derived attenuation maps: multicenter clinical trial with angiographic correlation. J Nucl Cardiol. 2005;12:676–86.
13. Gallowitsch HJ, Sykora J, Mikosch P, Kresnik E, Unterweger O, Molnar M, et al. Attenuation-corrected thallium-201 single-photon emission tomography using a gadolinium-153 moving line source: clinical value and the impact of attenuation correction on the extent and severity of perfusion abnormalities. Eur J Nucl Med. 1998;25:220–8.
14. Hung MC, Chang PW, Hsieh WA, Hwang JJ. Myocardial perfusion scintigraphy in Taiwan from 2005 to 2009. Nucl Med Commun. 2012;33:733–8.
15. Shibutani T, Onoguchi M, Yoneyama H, Konishi T, Matsuo S, Nakajima K, et al. Characteristics of single- and dual-photopeak energy window acquisitions with thallium-201 IQ-SPECT/CT system. Ann Nucl Med. 2017;31:529–35.
16. Xiao J, de Wit TC, Zbijewski W, Staelens SG, Beekman FJ. Evaluation of 3D Monte Carlo-based scatter correction for 201Tl cardiac perfusion SPECT. J Nucl Med. 2007;48:637–44.
17. Harel F, Genin R, Daou D, Lebtahi R, Delahaye N, Helal BO, et al. Clinical impact of combination of scatter, attenuation correction, and depth-dependent resolution recovery for (201)Tl studies. J Nucl Med. 2001;42:1451–6.
18. Wu YT, Chien CL, Wang SY, Yang WS, Wu YW. Gender differences in myocardial perfusion defect in asymptomatic postmenopausal women and men with and without diabetes mellitus. J Womens Health. 2013;22:439–44.
19. Wang SY, Cheng MF, Hwang JJ, Hung CS, Wu YW. Sex-specific normal limits of left ventricular ejection fraction and volumes estimated by gated myocardial perfusion imaging in adult patients in Taiwan: a comparison between two quantitative methods. Nucl Med Commun. 2011;32:113–20.
20. Thompson R, Heller G, Johnson L, Case J, Cullom S, Garcia E, et al. Value of attenuation correction on ECG-gated SPECT myocardial perfusion imaging related to body mass index. J Nucl Cardiol. 2005;12:195–202.
21. Yamauchi Y, Kanzaki Y, Otsuka K, Hayashi M, Okada M, Nogi S, et al. Novel attenuation correction of SPECT images using scatter photopeak window data for the detection of coronary artery disease. J Nucl Cardiol. 2014;21:109–17.
22. Banzo I, Pena FJ, Allende RH, Quirce R, Carril JM. Prospective clinical comparison of non-corrected and attenuation- and scatter-corrected myocardial perfusion SPECT in patients with suspicion of coronary artery disease. Nucl Med Commun. 2003;24:995–1002.
23. Klocke FJ, Baird MG, Lorell BH, Bateman TM, Messer JV, Berman DS, et al. ACC/AHA/ASNC guidelines for the clinical use of cardiac radionuclide imaging–executive summary: a report of the American College of Cardiology/American Heart Association Task Force on Practice Guidelines (ACC/AHA/ASNC Committee to Revise the 1995 Guidelines for the Clinical Use of Cardiac Radionuclide Imaging). J Am Coll Cardiol. 2003;42:1318–33.
24. Chien CL, Wu YW, Yang WS, Yang PC, Su HM, Wu YT. Myocardial perfusion image in asymptomatic postmenopausal women with physical inactivity and overweight. Obesity Facts. 2011;4:372–8.
25. Apostolopoulos DJ, Gąsowska M, Savvopoulos CA, Skouras T, Spyridonidis T, Andrejczuk A, et al. The impact of transmission-emission misregistration on the interpretation of SPET/CT myocardial perfusion studies and the value of misregistration correction. Hell J Nucl Med. 2015;18:114–21.
26. Ogawa K, Harata Y, Ichihara T, Kubo A, Hashimoto S. A practical method for position-dependent Compton-scatter correction in single photon emission CT. IEEE Trans Med Imaging. 1991;10:408–12.
27. Segmentation AHAWGoM, Imaging: RfC, Cerqueira MD, Weissman NJ, Dilsizian V, Jacobs AK, et al. Standardized myocardial segmentation and nomenclature for tomographic imaging of the heart: a statement for healthcare professionals from the cardiac imaging committee of the council on clinical cardiology of the american heart association. Circulation. 2002;105:539–42.
28. Brodov Y, Frenkel A, Chouraqui P, Przewloka K, Rispler S, Abadi S, et al. Influence of attenuation correction on transient left ventricular dilation in dual isotope myocardial perfusion imaging in patients with known or suspected coronary artery disease. Am J Cardiol. 2012;110:57–61.

29. Hart PD. Receiver operating characteristic (ROC) curve analysis: a tutorial using body mass index (BMI) as a measure of obesity. J Phys Act Res. 2016;1:5–8.
30. Ortiz-Perez JT, Meyers SN, Lee DC, Kansal P, Klocke FJ, Holly TA, et al. Angiographic estimates of myocardium at risk during acute myocardial infarction: validation study using cardiac magnetic resonance imaging. Eur Heart J. 2007;28:1750–8.
31. Donato P, Coelho P, Santos C, Bernardes A, Caseiro-Alves F. Correspondence between left ventricular 17 myocardial segments and coronary anatomy obtained by multi-detector computed tomography: an ex vivo contribution. Surg Radiol Anat. 2012;34:805–10.
32. Kosinski AS. A weighted generalized score statistic for comparison of predictive values of diagnostic tests. Stat Med. 2013;32:964–77.
33. Hwang LC, Bai CH, Chen CJ. Prevalence of obesity and metabolic syndrome in Taiwan. J Formos Med Assoc. 2006;105:626–35.
34. Hachamovitch R, Hayes SW, Friedman JD, Cohen I, Berman DS. Stress myocardial perfusion single-photon emission computed tomography is clinically effective and cost effective in risk stratification of patients with a high likelihood of coronary artery disease (CAD) but no known CAD. J Am Coll Cardiol. 2004;43:200–8.
35. Johansen A, Grupe P, Veje A, Braad PE, Hoilund-Carlsen PF. Scatter and attenuation correction changes interpretation of gated myocardial perfusion imaging. Eur J Nucl Med Mol Imaging. 2004;31:1152–9.
36. Benkiran M, Mariano-Goulart D, Bourdon A, Sibille L, Bouallegue FB. Is computed tomography attenuation correction more efficient than gated single photon emission computed tomography analysis in improving the diagnostic performance of myocardial perfusion imaging in patients with low prevalence of ischemic heart disease? Nucl Med Commun. 2015;36:69–77.
37. Links JM, DePuey EG, Taillefer R, Becker LC. Attenuation correction and gating synergistically improve the diagnostic accuracy of myocardial perfusion SPECT. J Nucl Cardiol. 2002;9:183–7.
38. Liu CJ, Cheng JS, Chen YC, Huang YH, Yen RF. A performance comparison of novel cadmium-zinc-telluride camera and conventional SPECT/CT using anthropomorphic torso phantom and water bags to simulate soft tissue and breast attenuation. Ann Nucl Med. 2015;29:342–50.
39. Kennedy JA, Brodov Y, Weinstein AL, Israel O, Frenkel A. The effect of CT-based attenuation correction on the automatic perfusion score of myocardial perfusion imaging using a dedicated cardiac solid-state CZT SPECT/CT. J Nucl Cardiol. 2017. https://doi.org/10.1007/s12350-017-0905-0.
40. Caobelli F, Akin M, Thackeray JT, Brunkhorst T, Widder J, Berding G, et al. Diagnostic accuracy of cadmium-zinc-telluride-based myocardial perfusion SPECT: impact of attenuation correction using a co-registered external computed tomography. Eur Heart J Cardiovasc Imaging. 2016;17:1036–43.
41. van Dijk JD, Mouden M, Ottervanger JP, van Dalen JA, Knollema S, Slump CH, et al. Value of attenuation correction in stress-only myocardial perfusion imaging using CZT-SPECT. J Nucl Cardiol. 2017;24:395–401.
42. Sciagra R. The expanding role of left ventricular functional assessment using gated myocardial perfusion SPECT: the supporting actor is stealing the scene. Eur J Nucl Med Mol Imaging. 2007;34:1107–22.
43. Linden A. Measuring diagnostic and predictive accuracy in disease management: an introduction to receiver operating characteristic (ROC) analysis. J Eval Clin Pract. 2006;12:132–9.
44. Hendel RC, Berman DS, Cullom SJ, Follansbee W, Heller GV, Kiat H, et al. Multicenter clinical trial to evaluate the efficacy of correction for photon attenuation and scatter in SPECT myocardial perfusion imaging. Circulation. 1999;99:2742–9.
45. Shotwell M, Singh BM, Fortman C, Bauman BD, Lukes J, Gerson MC. Improved coronary disease detection with quantitative attenuation-corrected Tl-201 images. J Nucl Cardiol. 2002;9:52–62.
46. Wu YW, Chen YH, Wang SS, Jui HY, Yen RF, Tzen KY, et al. PET assessment of myocardial perfusion reserve inversely correlates with intravascular ultrasound findings in angiographically normal cardiac transplant recipients. J Nucl Med. 2010;51:906–12.
47. Liu CJ, Wu YW, Ko KY, Chen YC, Cheng MF, Yen RF, et al. Incremental diagnostic performance of combined parameters in the detection of severe coronary artery disease using exercise gated myocardial perfusion imaging. PLoS ONE. 2015;10:e0134485.